Supporting Information

Excitation Wavelength Dependent Photon Anti-bunching/Bunching from Single Quantum Dots near Gold Nanostructures

Swayandipta Dey[†], *Yadong Zhou*[‡], *Yonglei Sun*[#], *Julie A. Jenkins*[†], *David Kriz*[†], *Steven L. Suib*[†#], *Ou Chen*[§], *Shengli Zou*[‡], *Jing Zhao*[†#*]

[†]Department of Chemistry, University of Connecticut, 55 North Eagleville Rd, Storrs, CT, 06269-3060, USA

[‡]Department of Chemistry, University of Central Florida, 4111 Libra Drive, Orlando, Florida 32816-2366, USA

[#]Institute of Materials Science, University of Connecticut, Storrs, CT, 06269-3136, USA

[§] Department of Chemistry, Brown University, Providence, RI 02912, USA

*Corresponding author: Department of Chemistry, University of Connecticut, 55 North Eagleville Rd, Storrs, CT, 06269-3060, USA, Phone: 860-486-2443, Fax: 860-486-2981 Email: jing.zhao@uconn.edu

1. Experimental Methods

1.1 LSPR Substrate Preparation and Characterization

Gold nanoparticles (Au NPs) with diameter of approximately 120 nm was synthesized using a two-step seed-mediated method as reported earlier.[1] The as-synthesized Au NPs were incubated on glass substrates which were pretreated with aminopropyltriethoxysilane. Details on substrate preparation for the optical studies has been described in our earlier study.[2-3] In order to prevent complete quenching of the fluorescence of the quantum dots, the Au NP substrates were coated with a dielectric alumina spacer. A ~20 nm thick alumina layer was deposited on the Au NP substrates using atomic layer deposition. The thickness of alumina was calculated based on a layer-by-layer growth of alumina with an average growth rate ∼1 Å/cycle. A home-built LSPR setup was used to measure the extinction spectra of the immobilized Au NPs on the glass substrate. The scanning electron microscopy (SEM) image of dielectric alumina modified Au NP substrates was obtained using a JEOL JSM-6330F scanning electron microscope (SEM) operated at 15 kV.

1.2 QD Synthesis and Characterization

CdSe/CdS core/shell QDs were synthesized following the procedure developed by Chen et al.[4] The photoluminescence (PL) quantum yield (QY) of the QDs dispersed in hexane is 94.9%, as determined by comparison to Rhodamine B in ethanol. The shape and size distribution of the QDs was characterized using a JEOL2010 transmission electron microscope (TEM) operated at 200 kV. The absorption and ensemble solution photoluminescence spectra of the QDs were collected using Cary-60 (Agilent) UV-Vis spectrophotometer and spectrofluorometer (FluoMax Plus, Horiba Scientific) respectively.

1.3 Time-Resolved Photoluminescence Measurements

Single particle optical measurements were performed using a home-built confocal epifluorescence Nikon Ti-U microscope equipped with a piezo-scanning XYZ-stage (PI 320, Physik Instrumente). A supercontinuum pulsed laser (Solea, PicoQuant, ~100-120 ps pulse duration, 2.5 MHz repetition rate) was used to excite the QDs at 510 nm, 530 nm, 550 nm and 580 nm. The PL of the samples was collected through a 100x oil-immersion objective (N.A.=1.3). The emitted light was allowed to pass through a non-polarizing beam-splitter and spectrally filtered using 630/60 nm band-pass filters. The light was then directed onto two single photon detectors (τ-SPAD, Pico-Quant) arranged in Hanbury-Brown Twiss geometry. Time-dependent photon correlation function $g^2(\tau)$ and PL intensity-time traces of individual QDs both on glass and on Au NP substrates were collected using a time correlated single photon counting system PicoHarp-300 (PicoQuant) operated in a time-tagged time-resolved (TTTR) mode with a timing resolution of 32 ps. All the measurements were performed at room temperature. The $g^2(\tau)$ data were processed with a commercial Sympho Time 64 software (Picoquant).The PL spectra of single QDs dispersed on glass or Au substrates were acquired by directing the emission signal to an spectrometer (IsoPlane SCT 320, Princeton Instruments) mounted with a charge coupled device (CCD, Pixis 1024, Princeton Instruments). All the measurements were performed at room temperature.

1.4. Theoretical modeling

The enhanced electric fields around metal nanoparticles are calculated using the discrete dipole approximation method. The detailed discussion about the method can be found in the previous paper by Draine et al.[5] The enhanced radiative and non-radiative rate of the QD when an Au NP is placed near to it are calculated using equations discussed in the previous report.[2, 6] The parameters in the equations are calculated using the discrete dipole approximation method. In the calculations, the dimension and configuration of the Au NP are the same as in the experiment and the dielectric constants of Au are taken from Palik's handbook.[7]

2. Calculations of average photons absorbed per excitation pulse, $\langle N \rangle$

The absorption cross-section $C_{abs}(\omega)$ of CdSe/CdS quantum dots(QDs) is calculated using the equations developed earlier by Leatherdale et al[8]:

$$C_{abs}(\omega) = \frac{\omega}{m_3 c}|\mathrm{f}(\omega)^2|2n_1k_1\frac{4}{3}\pi R^3 = \frac{1}{\lambda m_3}|\mathrm{f}(\omega)^2|2n_1k_1\frac{4}{3}\pi R^3 = \varsigma R^3$$

$$\mathrm{f}(\omega) = \frac{3m_3^2}{m_1^2+2m_3^2}$$

where n_1, k_1 are the real and imaginary part of the bulk absorption coefficient, R is the radius of the QD, and m_3 is the refractive index (R.I.) of the medium (Hexane, R.I. = 1.375 at 20 ºC). The parameter *f* is the local field factor where $m_1 = n_1 + ik_1$ is the complex R.I. of the QD.

For the core/shell QDs, the absorption cross-section is averaged over the QD volume as reported earlier:

$$C_{abs}(\omega) = \varsigma_{\omega}^{core} R_c^3 + \varsigma_{\omega}^{shell}[(R_C + T_S)^3 - R_C^3] = \varsigma_{\omega}^{shell}[(R_C + T_S)^3] + (\varsigma_{\omega}^{core} - \varsigma_{\omega}^{shell}) R_c^3$$

where R_C is the radius of the CdSe core, and T_S is the thickness of the CdS shell.

For the CdSe/CdS QDs, R_C = 1.5nm and T_S = 3nm, and the refractive indices of CdSe and CdS are obtained from Palik et al[7]:

Under 510 nm excitation, $\varsigma_{\omega}^{core} = 8.479 \times 10^4$ cm^{-1} and $\varsigma_{\omega}^{shell} = 7.001 \times 10^4$ cm^{-1}.

Under 580 nm excitation, $\varsigma_{\omega}^{core} = 6.136 \times 10^4$ cm^{-1} and $\varsigma_{\omega}^{shell} = 3.681 \times 10^4$ cm^{-1}.

Using the above equations for the absorption cross-section of the CdSe/CdS QDs, the calculated $C_{abs}(510\ nm) = 6.428 \times 10^{-15}$ cm^2 and $C_{abs}(580\ nm) = 3.437 \times 10^{-15}$ cm^2.

For the single QD measurements, we assume the spot size to be diffraction limited.

Therefore, the spot size can be calculated as $\frac{1.22 \times \lambda}{NA}$ (where NA = 1.30 for the objective used). The calculated spot size is 7.196×10^{-9} cm^2 at 510 nm, and is 9.307×10^{-9} cm^2 at 580 nm.

Therefore, the average number of photons absorbed per excitation pulse can be calculated as $\langle N \rangle = \frac{C_{abs} \times excitation\ power}{E_{photon} \times spot\ size \times laser\ repetition\ rate}$

At 580 nm excitation, for excitation powers of 50 nW, 100 nW, 250 nW, 500 nW and 1000 nW, the calculated values of $\langle N \rangle$ are 0.02, 0.10, 0.21, 0.42 and 1.05.

3. Interpretation of $g_0^{(2)}$

A QD absorbs a number of N photons from one excitation pulse. Let ξ_m be a random variable that equals to 1, if the decay of the *m* multiexcitonic state to the *m-1* multiexcitonic state in the *N*-length recombination cascade is radiative; and equals to 0 if that process is nonradiative. We notice that $\xi_m^2 = \xi_m$.

The emitted photon number during the same pulse, *n*, can be expressed by

$$\mathrm{n} = \sum_{m=1}^{N} \xi_m$$

From previous literature[9-10], under low detection efficiency limit, $g_0^{(2)}$ is given by

$$g_0^{(2)} = \frac{\langle n(n-1)\rangle}{\langle n^2\rangle}$$

Where $\langle n\rangle$ denotes the average value. Use the fact that ξ_m^2=ξ_m, we have

$$\mathrm{n(n-1)} = \sum_{m=1}^{N} \xi_m \left(\sum_{m'=1}^{N} \xi_{m'} - 1 \right) = \left(\sum_{m=1}^{N} \xi_m \right)^2 - \sum_{m=1}^{N} \xi_m$$

$$= \sum_{m=1}^{N} {\xi_m}^2 + 2\sum_{m'<m}^{N} \xi_m\, \xi_{m'} - \sum_{m=1}^{N} \xi_m = 2\sum_{m'<m}^{N} \xi_m\, \xi_{m'}$$

Therefore

$$g_0^{(2)} = \frac{\langle n(n-1)\rangle}{\langle n^2\rangle} = \frac{2\sum_m^N P_{N\geq m} \sum_{m'<m} \langle \xi_m \xi_{m'}\rangle}{\left(\sum_m^N P_{N\geq m} \langle \xi_m\rangle\right)^2}$$

Where $P_{N\geq m}$ denotes the possibility that at least *m* photons are absorbed by the QD. Since the absorption process can be treated as Poissonian, i.e., $P_{N=m} = \frac{N^m}{m!}\exp(-\langle N\rangle)$, $P_{N\geq m}$ can be determined by $P_{N\geq m} = 1 - \sum_i^{m-1} P_{N=i}$.

If only the biexciton and exciton emissions are considered (when the excitation power is moderate), then $g_0^{(2)}$ can be approximated by

$$g_0^{(2)} \sim \frac{2P_{n\geq 2}\langle \xi_2 \xi_1\rangle}{P_{N\geq 1}^2 \langle \xi_1\rangle^2} = \frac{2[1-\exp(-\langle N\rangle) - \langle N\rangle \exp(-\langle N\rangle)]}{[1-\exp(-\langle N\rangle)]^2} \cdot \frac{\langle \xi_2 \xi_1\rangle}{\langle \xi_1\rangle^2}$$

Considering the independence of biexciton and exciton emissions, i.e., $\langle \xi_2 \xi_1\rangle = \langle \xi_2\rangle\langle \xi_1\rangle$,[1] and noticing that $\langle \xi_1\rangle = \eta_X$, $\langle \xi_2\rangle = \eta_{BX}$ we have

$$g_0^{(2)} \sim \frac{2P_{n\geq 2}}{P_{N\geq 1}^2} \cdot \frac{\langle \xi_2 \rangle}{\langle \xi_1 \rangle} = \frac{2P_{n\geq 2}}{P_{N\geq 1}^2} \cdot \frac{\eta_{BX}}{\eta_X} = \frac{2[1 - \exp(-\langle N \rangle) - \langle N \rangle \exp(-\langle N \rangle)]}{[1 - \exp(-\langle N \rangle)]^2} \cdot \frac{\eta_{BX}}{\eta_X}$$

This equation is still valid when the QD is placed near plasmonic nanostructures. In that case, replace $\langle N \rangle_{eff}$ with $\langle N \rangle$, and replace η_X' (η_{BX}') with η_X (η_{BX}):

$$g_0^{(2)} \sim \frac{2[1 - \exp\left(-\langle N_{eff} \rangle\right) - \langle N_{eff} \rangle \exp\left(-\langle N_{eff} \rangle\right)]}{[1 - \exp(-\langle N_{eff} \rangle)]^2} \cdot \frac{\eta_{BX}'}{\eta_X'}$$

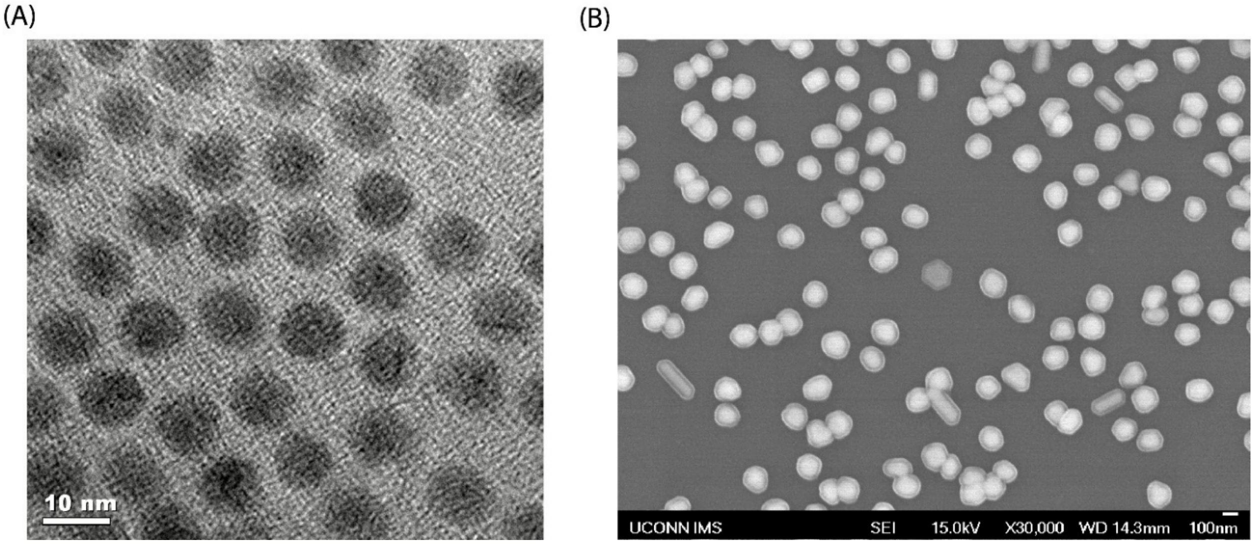

Figure S1. (A) HR-TEM image of CdSe/CdS QDs with an average calculated diameter of 9.2 ± 1.2 nm. (B) SEM image of ~ 120 nm gold nanoparticle coated 20 nm alumina on glass.

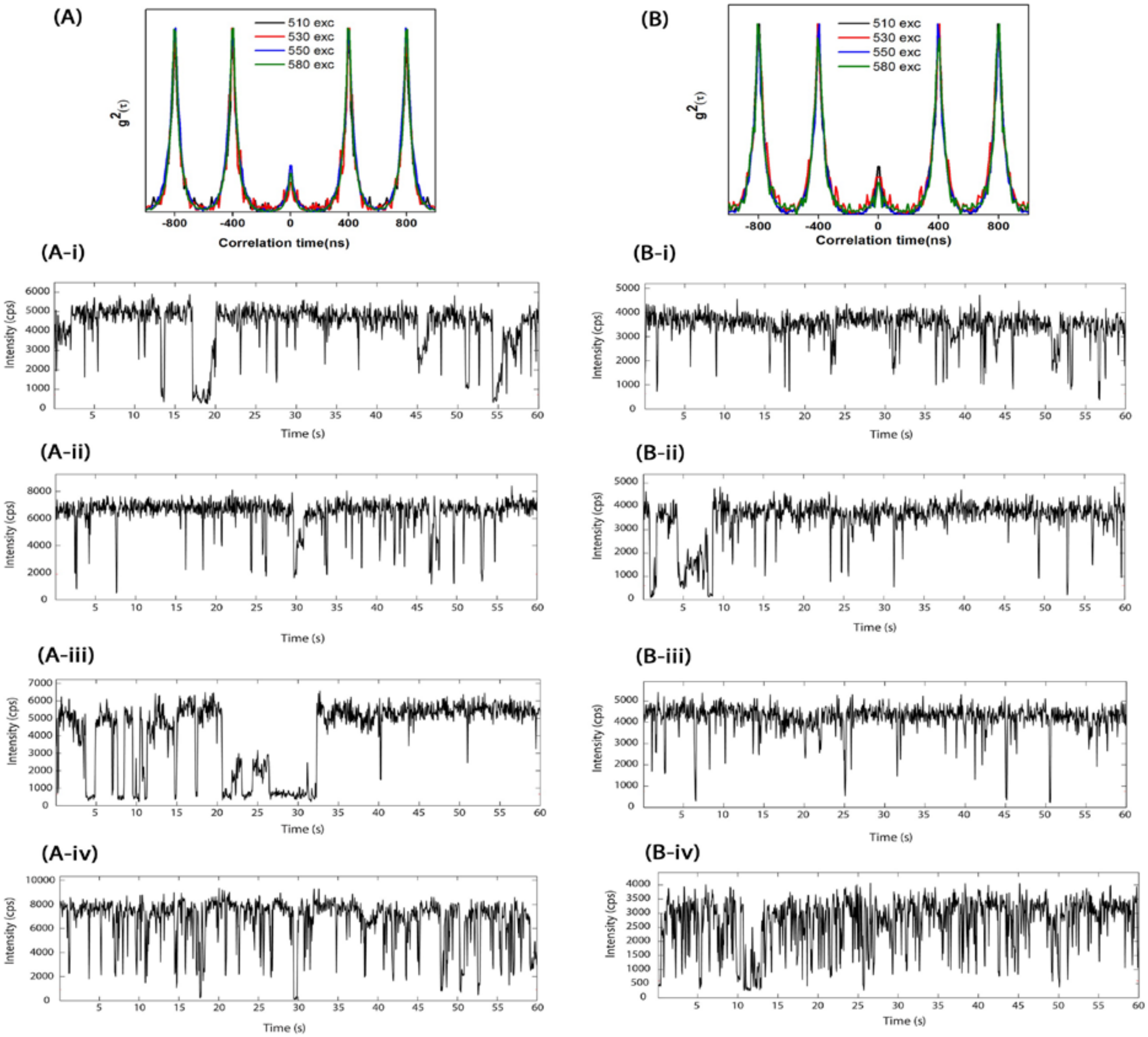

Figure S2. (A, B) Representative $g^{(2)}$ functions and (A,B -i, ii, iii, iv) PL time traces of two individual QDs deposited on glass under excitation wavelengths of 510, 530, 550 and 580 nm.

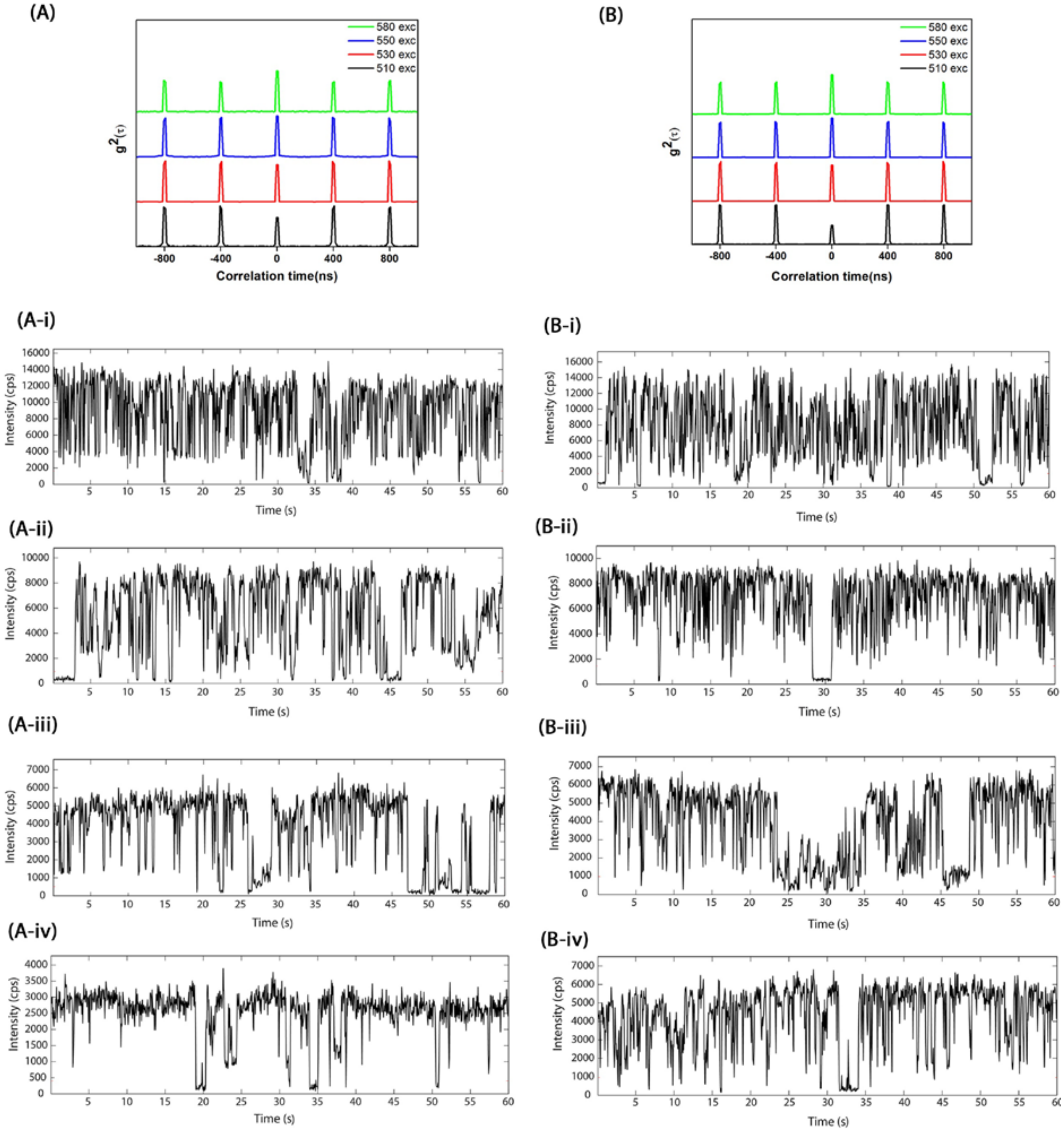

Figure S3. (A, B) Representative $g^{(2)}$ functions and (A,B -i, ii, iii, iv) PL time traces of two individual QDs deposited on Au NP substrates measured under excitation wavelengths of 510, 530, 550 and 580 nm.

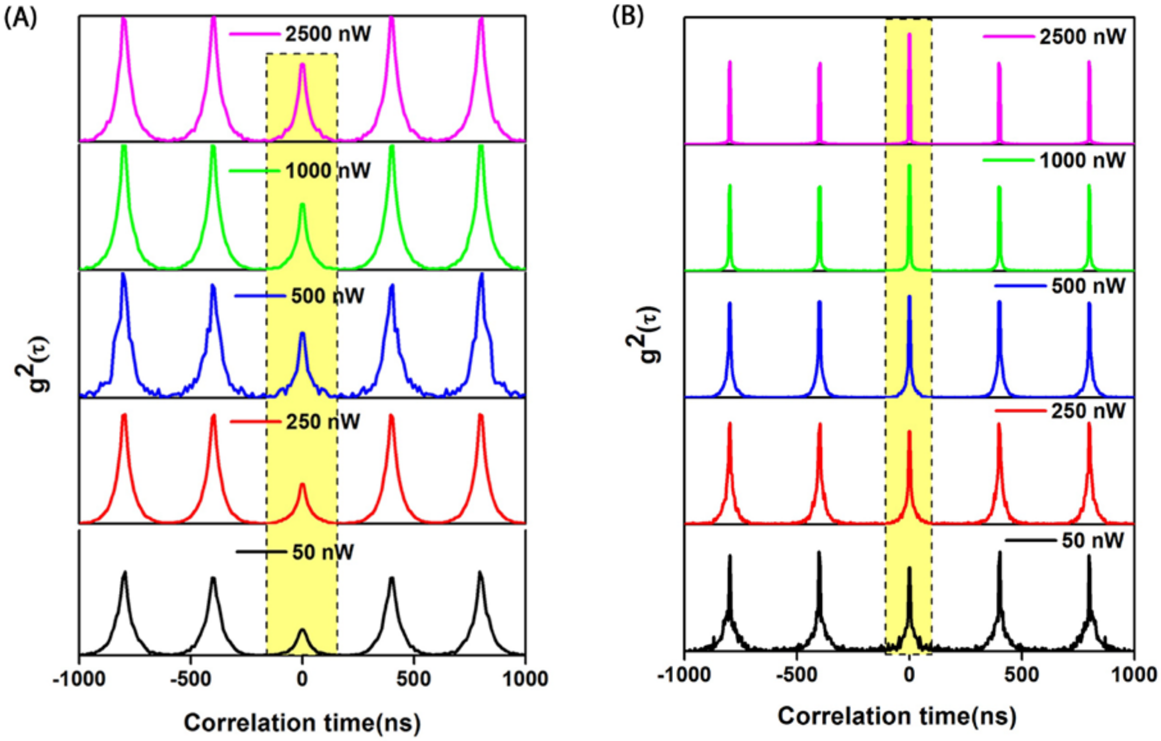

Figure S4. Representative photon correlation histograms at 580 nm excitation showing excitation pump power dependence of $g^{(2)}$ functions for individual QDs deposited on (A) glass and (B) Au NP substrates. The shaded portions in the histograms indicate the difference in multiexciton emission behavior of individual QD under different excitation power as observed from the steep rise in center peak (at $\tau = 0$) when the excitation wavelength overlaps with the LSPR of Au NPs.

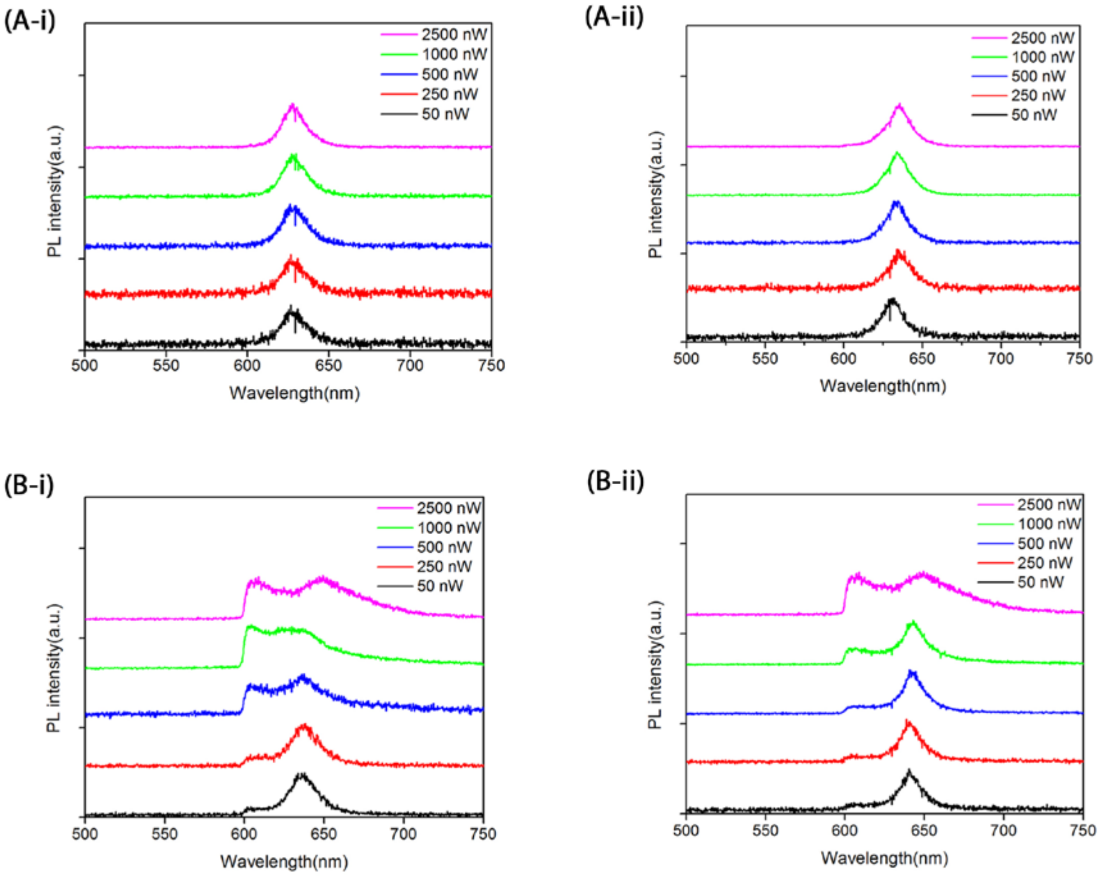

Figure S5. Representative single QD PL emission spectra collected at 580 nm excitation with different powers at (50 nW,250 nW,500 nW,1000 nW and 2500 nW) on (A-i and ii) glass and (B-i and ii) Au NP substrates.

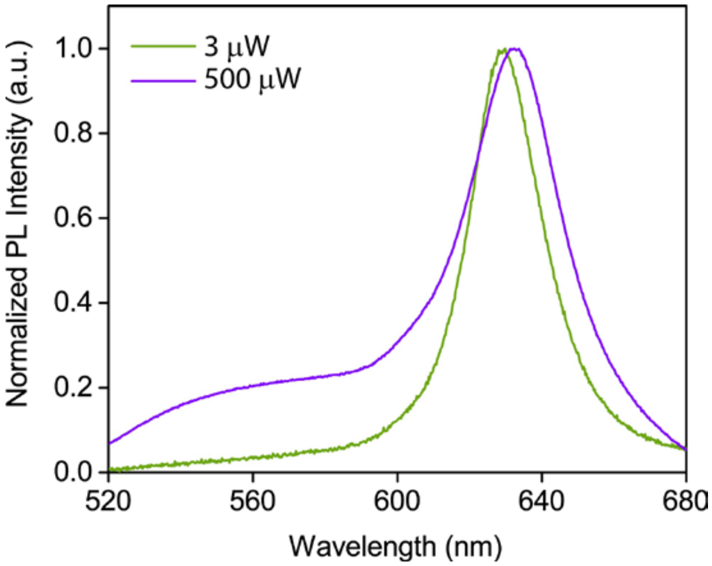

Figure S6. PL spectra of a single QD on a glass substrate collected at 490 nm excitation with excitation powers of 3 μW (green) and 500 μW (purple).

Reference:

1. Kimling, J.; Maier, M.; Okenve, B.; Kotaidis, V.; Ballot, H.; Plech, A. Turkevich Method for Gold Nanoparticle Synthesis Revisited. *J. Phys. Chem. B* **2006,** *110* (32), 15700-15707.
2. Dey, S.; Zhou, Y.; Tian, X.; Jenkins, J. A.; Chen, O.; Zou, S.; Zhao, J. An experimental and theoretical mechanistic study of biexciton quantum yield enhancement in single quantum dots near gold nanoparticles. *Nanoscale* **2015,** *7* (15), 6851-6858.
3. Jenkins, J. A.; Zhou, Y.; Thota, S.; Tian, X.; Zhao, X.; Zou, S.; Zhao, J. Blue-Shifted Narrow Localized Surface Plasmon Resonance from Dipole Coupling in Gold Nanoparticle Random Arrays. *J. Phys. Chem. C* **2014,** *118* (45), 26276-26283.
4. Chen, O.; Zhao, J.; Chauhan, V. P.; Cui, J.; Wong, C.; Harris, D. K.; Wei, H.; Han, H.-S.; Fukumura, D.; Jain, R. K.; Bawendi, M. G. Compact high-quality CdSe–CdS core–shell nanocrystals with narrow emission linewidths and suppressed blinking. *Nat. Mater.* **2013,** *12* (5), 445-451.
5. Draine, B. T. The discrete-dipole approximation and its application to interstellar graphite grains. *Astrophys. J.* **1988,** *333* (Oct.15), 848-872.
6. Wang, H.; Zou, S. A generalized electrodynamics model for surface enhanced Raman scattering and enhanced/quenched fluorescence calculations. *RSC Adv.* **2013,** *3* (44), 21489-21493.
7. Palik, E.D. *Handbook of Optical Constants of Solids III*, **1991,** Academic Press, Boston.
8. Leatherdale, C. A.; Woo, W. K.; Mikulec, F. V.; Bawendi, M. G. On the Absorption Cross Section of CdSe Nanocrystal Quantum Dots. *J. Phys. Chem. B* **2002,** *106* (31), 7619-7622.
9. Nair, G.; Zhao, J.; Bawendi, M. G. Biexciton Quantum Yield of Single Semiconductor Nanocrystals from Photon Statistics. *Nano Lett.* **2011,** *11* (3), 1136-1140.
10. Park, Y.-S.; Ghosh, Y.; Chen, Y.; Piryatinski, A.; Xu, P.; Mack, N. H.; Wang, H.-L.; Klimov, V. I.; Hollingsworth, J. A.; Htoon, H. Super-Poissonian Statistics of Photon Emission from Single CdSe-CdS Core-Shell Nanocrystals Coupled to Metal Nanostructures. *Phys. Rev. Lett.* **2013,** *110* (11), 117401.